THE JOURNAL OF PHYSICAL CHEMISTRY B

Article

pubs.acs.org/JPCB

Interaction of Celecoxib with Membranes: The Role of Membrane Biophysics on its Therapeutic and Toxic Effects

Catarina Pereira-Leite, Cláudia Nunes,* José L. F. C. Lima, Salette Reis, and Marlene Lúcio

REQUIMTE, Departamento de Ciências Químicas, Faculdade de Farmácia, Universidade do Porto, Portugal

ABSTRACT: The present work provides a biophysical characterization of the interaction of celecoxib, a cyclo-oxigenase-2 selective nonsteroidal anti-inflammatory drug, with membranes using liposomes, constituted by phosphatidylcholines, as membrane model systems. In order to mimic biological conditions, the experiments were performed at physiological pH (7.4); at an acidic pH to mimic the conditions of the inflamed cells (5.0); and at different membrane physical states (gel, ripple, and fluid phase). Important information regarding the celecoxib–membrane interactions was gathered by the complementary biophysical techniques: derivative spectrophotometry was used to determine liposome/water partition coefficient of celecoxib; dynamic light scattering (DLS) measurements were performed to study the influence of celecoxib on lipid main phase transition temperature; fluorescence binding measurements were made to assess the location of celecoxib within the membrane; and small-angle and wide-angle X-ray scattering (SAXS and WAXS) were used to assess the changes in the structure and order of phosphatidylcholine bilayers caused by the presence of celecoxib. The overall results obtained indicate that celecoxib greatly interacts with membranes. Briefly, celecoxib exhibits a high liposome/water partition coefficient that is non-pH-dependent, but the location of celecoxib within the membrane is pH-dependent. In fact, celecoxib is more deeply located inside the membrane at pH 5.0, while it locates closer to the surface at pH 7.4. DLS, SAXS, and WAXS results have shown a high membrane fluidization in the presence of celecoxib, especially at pH 7.4. Overall, the current study can contribute to a biophysical characterization of the celecoxib–membrane interaction. The relevance of the gathered results will be discussed in terms of the reported celecoxib therapeutic and toxic effects.

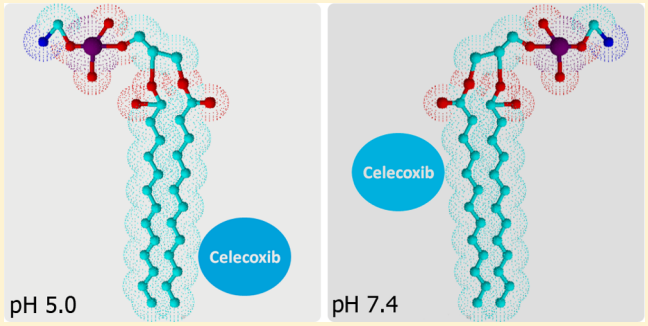

INTRODUCTION

Celecoxib is a cyclo-oxigenase-2 (COX-2) selective non-steroidal anti-inflammatory drug (NSAID) widely used in the treatment of osteoarthritis, rheumatoid arthritis, ankylosing spondylitis, acute pain in adults and familial adenomatous polyposis.[1] The main mechanism of action of celecoxib results from the inhibition of the production of prostaglandins by interacting with a membrane protein, COX-2. The selectivity of celecoxib to isoform 2 of COX avoids the typical gastrointestinal injuries caused by nonselective NSAIDs. Indeed, controlled studies suggested that coxibs (COX-2 selective NSAIDs) are associated with a lower incidence of serious gastrointestinal damage.[2] Although this represents a major advantage compared with nonselective NSAIDs, it was described that coxibs are not totally safe for the gastrointestinal (GI) tract, especially if used in chronic conditions, and in addiction, they have been associated with a dose-dependent increase of the risk of adverse cardiovascular effects, such as myocardial infarction, stroke, and heart failure.[2,3] In fact, the celecoxib mode of action depends directly on the drug interaction with the components of biological membranes. The COX active site, for instance, is at the end of a lipophilic channel, and this channel has its opening in the membrane interior, and thus, it is expected that membranes will be the first level of interaction of celecoxib before it enters the active site of COX. Furthermore, celecoxib GI and cardiovascular toxicity may also be a result of the drug–membrane interplay,[4] as the direct effects of NSAIDs on the biophysical properties of membranes can also have serious consequences affecting membrane integrity as a protective barrier.[5−8] Moreover, by causing changes in the lipid environment, NSAIDs may also affect enzyme function.[9,10] Therefore, the interaction of celecoxib with membranes plays an important role in understanding both its therapeutic and adverse effects.

In this context, this work is focused on the biophysical characterization of the interaction of celecoxib with liposomes composed by 1,2-dimyristoyl-*sn*-glycero-3-phosphocholine (DMPC) and 1,2-dipalmitoyl-*sn*-glycero-3-phosphocholine (DPPC). Since phosphatidylcholines are among the most abundant phospholipids of natural plasma membranes,[11] DMPC and DPPC were chosen to yield membrane mimetic models. Their structural similarity (except hydrophobic tail length) permits to obtain analogous and complementary information from both DMPC and DPPC vesicles. Furthermore, DPPC is an endogenous component of the joints and represents around 45% of the total synovial fluid lipid

Received: April 26, 2012
Revised: October 18, 2012

   dx.doi.org/10.1021/jp304037v | *J. Phys. Chem. B* XXXX, XXX, XXX–XXX

component, which is the main target of many inflammatory diseases.[12] In addition, phosphatidylcholines are typically used to analyze the physical−chemical and biological properties of cellular membranes.[13−15] The use of membrane model systems permits to assess easily the drug−membrane interaction by mimicking biological membrane constitution and dimensionality and reducing molecular complexity.

Since this is a biomimetic study, it is important to ensure that experimental conditions are close to those found by celecoxib in the course of its *in vivo* activity. Therefore, studies were performed at two different pH values: 7.4 to mimic the plasma pH and 5.0 to simulate inflamed cells pH.[16] In fact, the acid−base conditions are determinant to NSAIDs−membrane interaction, since different ionization states of celecoxib can be found in different pH environments, and usually, a higher degree of ionization corresponds to a weaker interaction with the membrane. In addition, considering the lipid polymorphism encountered by the drug at the membrane level, the studies were conducted in both its tilted gel phase ($L_{\beta'}$) and fluid phase (L_α). Although the fluid phase is the most biologically relevant, ordered domains, which shares common properties with the lipid gel phase,[11] are also present in membranes, and despite their important biological role, they are usually not taken into consideration when performing drug−membrane interaction studies.

In order to obtain a characterization of the celecoxib interaction with membranes, it is also important to use a wide range of biophysical techniques that offer complementary information. In this regard, liposomes were used to determine the partition coefficient of celecoxib between lipid and aqueous phases by derivative spectrophotometry. The location of celecoxib within the membrane bilayer was also studied by measuring relative fluorescence quenching efficiencies of DMPC vesicles labeled with either 1-palmitoyl-2-stearoyl-(5-DOXYL)-*sn*-glycero-3-phosphocholine (5-DOXYL) or 1-palmitoyl-2-stearoyl-(10-DOXYL)-*sn*-glycero-3-phosphocholine (10-DOXYL) with respect to celecoxib's fluorescence. Comparison of the quenching efficiencies allowed an estimation of the average depth location of celecoxib using the parallax method of analysis.[17,18] The influence of celecoxib on the main phase transition temperature of DMPC was further assessed by dynamic light scattering (DLS). In addition, structural information of DPPC bilayers was obtained by using small- and wide-angle X-ray scattering techniques (SAXS and WAXS). These techniques permitted the evaluation at a molecular level of the influence of celecoxib in the structural and packing parameters of model membranes.[19]

The results of the present work contribute to identifying celecoxib-induced alterations on membrane lipid physical properties putatively correlated with the pharmacological and toxic effects of celecoxib and may provide significant insights for predicting or modulating the impact of other more effective and less toxic drugs. Despite this, the biophysical complementary approach to clarify the therapeutic and toxic effects of celecoxib has not been undertaken before, and to our knowledge, this is the first report on celecoxib−membrane interactions.

EXPERIMENTAL METHODS

Materials. The lipids 1,2-dimyristoyl-*sn*-glycero-3-phosphocholine (DMPC) and 1,2-dipalmitoyl-*sn*-glycero-3-phosphocholine (DPPC) were obtained from Sigma-Aldrich Co. (St. Louis, MO, USA) and Avanti Polar Lipids, Inc. (Alabama, USA), respectively. Celecoxib was kindly provided by Pfizer Pharmaceutics (New York, USA). The probes 1-palmitoyl-2-stearoyl-(5-DOXYL)-*sn*-glycero-3-phosphocholine (5-DOXYL) and 1-palmitoyl-2-stearoyl-(10-DOXYL)-*sn*-glycero-3-phosphocholine (10-DOXYL) were obtained from Avanti Polar Lipids, Inc. (Alabama, USA). HEPES hemisodium salt was supplied by Sigma-Aldrich Co. (St. Louis, MO, USA). All other chemicals were obtained from Merck (Darmstadt, Germany). All reagents were used without further purification.

Celecoxib stock solutions were prepared in methanol. The buffers hepes (pH 7.4) or acetate (pH 5.0) were prepared with double-deionized water (conductivity less than 0.1 μS cm^{-1}) from a Millipore system, and the ionic strength (I = 0.1 M) was adjusted with NaCl.

Preparation of Liposomes. Liposomes were prepared according to a previously described method.[20−22] Briefly, the lipid, DMPC, was solubilized in a chloroform/methanol (3:2, v/v) mixture. Afterward, the organic solvents were evaporated under a nitrogen stream to obtain a dried lipid film without traces of organic solvents. The resultant dried lipid film was hydrated with an adequate volume of buffer (hepes or acetate) at 30 °C (temperature above the main phase transition temperature of the lipid) and vortexed to yield multilamellar vesicles (MLVs). Large unilamellar vesicles (LUVs) were then prepared by extrusion of the MLVs suspension through polycarbonate filters with a pore size of 100 nm at 30 °C.

In order to prepare labeled liposomes, the probe (either 5-DOXYL or 10-DOXYL) was previously dissolved in chloroform and co-dried with the lipid by evaporating the solvents. The probe was always incorporated to give a probe/lipid molar ratio of 1:6 (previously determined to ensure a complete incorporation of the probe in the lipid vesicles).

Determination of Partition Coefficients by Derivative Spectrophotometry. The partition coefficient (K_p) of celecoxib between liposomes and a aqueous phase (acetate or hepes buffer to obtain pH 5.0 and pH 7.4, respectively) was determined by derivative spectrophotometry, as described in previous works.[14,20,23] Samples were prepared from LUVs with increasing concentrations of DMPC (0−1000 μM) and a fixed concentration of celecoxib (20 μM). The correspondent reference suspensions were similarly prepared in the absence of drug. All the suspensions were incubated at 30 °C during 30 min. A Jasco V-660 spectrophotometer was used to obtain the absorbance spectra of samples and references in the range 220−570 nm in the fluid phase (L_α) of DMPC (30 °C). The results were mathematically treated, using a developed routine, *Kp Calculator*.[24] This treatment consists of (i) subtracting the reference absorption spectrum to the correspondent sample absorption spectrum to obtain corrected absorption spectra; (ii) calculating the second- and third-derivative spectra to eliminate the light scattering caused by the presence of liposomes, enhancing the detection of minor spectral features and improving the resolution of bands; (iii) determining the partition coefficient from the third derivative spectra at the wavelength where the scattering was eliminated, by fitting eq 1 to the experimental data (D_T versus [L]) using a nonlinear least-squares regression method where the adjustable parameter is the partition constant, K_p:

$$D_T = D_w + \frac{(D_m - D_w)K_p[L]V_m}{1 + K_p[L]V_m} \quad (1)$$

dx.doi.org/10.1021/jp304037v | J. Phys. Chem. B XXXX, XXX, XXX−XXX

In this equation, D is the third derivative intensity ($D = d^n Abs/d\lambda^n$) obtained from the absorbance values of the total amount of celecoxib (D_T), celecoxib distributed on the lipid membrane phase (D_m), and celecoxib distributed in the aqueous phase (D_w), respectively. [L] represents the lipid concentration (in M) and V_m is the lipid molar volume. For DMPC, V_m is 0.66 L mol^{-1} and the mean molecular weight is 677.93 g mol^{-1}.[25]

Phase Transition Temperature Studies by Dynamic Light Scattering. The main phase transition temperature and the cooperativity of DMPC vesicles in the presence and absence of celecoxib at pH 5.0 and 7.4 was determined by dynamic light scattering (DLS), as already described.[26] A fixed concentration of DMPC (500 μM) and celecoxib (20 μM) was used and the sample was incubated at 30 °C during 30 min. The experiments were performed in a BI-MAS DLS instrument (Brookhaven Instruments, USA) containing a controlled temperature cell holder. The samples were heated from 10 to 40 °C with intervals of 1 °C with an equilibration period of 2 min. At each temperature, 3 runs of 2 min were made. The results were collected as average count rate versus temperature and the data were fitted using eq 2:[27]

$$r_s = r_{s1} + p_1 T + \frac{r_{s2} - r_{s1} + p_2 T - p_1 T}{1 + 10^{B(1/T - 1/T_m)}} \quad (2)$$

where r_s is the average count rate, T is the temperature (°C), p_1 and p_2 are the slopes of the linear fits to the data before and after the phase transition region (respectively) and r_{s1} and r_{s2} are the corresponding y intercepts. This fitting also permits to obtain the cooperativity (B) and the main phase transition temperature (T_m) of the lipid bilayers from the gel phase to the fluid phase.

Fluorescence Binding Measurements. The celecoxib–membrane binding was assessed by a spectrofluorimetric titration technique. The DOXYL derivatives (5-DOXYL and 10-DOXYL) were used as quenchers, since they have the DOXYL group in a well-established location within the phospholipid membrane, and celecoxib, a fluorescent drug, was the fluorophore. The changes in celecoxib fluorescence intensity were followed as a function of drug concentration. The samples were incubated for 30 min at 30 °C so that celecoxib could reach the partition equilibrium between the lipid membranes and the aqueous phase. References were also prepared with liposomes without DOXYL group in the presence of the same concentrations of celecoxib. The studies were performed at pH 5.0 and 7.4 by using acetate or hepes buffer, respectively. The experiments were performed in a Jasco FP-6500 spectrofluorimeter containing a constant temperature cell holder, and the data were obtained on a 1 cm path length cuvette at a fixed temperature (30 °C) at which the lipid is in the liquid crystalline fluid phase. The excitation and emission wavelengths of celecoxib were set to 259 and 372 nm, respectively.

The intensity obtained with the samples was subtracted from the references and normalized to determine the binding of celecoxib to liposomes. These results were fitted using the eq 3:[28]

$$\Delta F = (\Delta F_{max}[\text{Celecoxib}]_m)/([\text{Celecoxib}]_m + K_D) \quad (3)$$

where ΔF is the normalized fluorescence intensity, ΔF_{max} is the maximum normalized fluorescence intensity, $[\text{Celecoxib}]_m$ is the membrane concentration of celecoxib, and K_D is the dissociation constant. The binding efficiency of celecoxib depends on the partition of celecoxib between the membrane and the aqueous phase, since the quenching will occur only if the drug is closely located to any of the DOXYL quenchers used. Therefore, the membrane concentration of celecoxib ($[\text{Celecoxib}]_m$) was calculated taking into account the total concentration of the drug ($[\text{Celecoxib}]_T$), the drug partition coefficient (K_p), and the phospholipid molar volume (V_m), as described by eq 4:

$$[\text{Celecoxib}]_m = \frac{K_p[\text{Celecoxib}]_T}{K_p V_m + (1 - V_m)} \quad (4)$$

Membrane Location Studies by Parallax Method of Depth-Dependent Fluorescence Quenching. The celecoxib location within the membrane was estimated by analyzing the binding measurements results with the parallax method described by eq 5:[18]

$$Z_{cf} = L_{c1} + \left[-\frac{\ln\left(\frac{F_1}{F_2}\right)}{\pi C} - L_{21}^2 \right] / 2L_{21} \quad (5)$$

where Z_{cf} is the distance of the fluorophore from the center of the bilayer, F_1 is the normalized fluorescence intensity in the presence of the shallower quencher (i.e., 5-DOXYL), F_2 is the normalized fluorescence intensity in the presence of the deeper quencher (i.e., 10-DOXYL), L_{c1} is the distance of the shallow quencher from the center of the bilayer, L_{21} is the distance between the shallow and deep quenchers, and C is the concentration of quencher in liposomes/Å^2 (mole fraction of DOXYL labeled phospholipid/area per phospholipid). F_1 and F_2 were determined by ΔF_{max} obtained from each binding experiment. L_{c1} and L_{c2} (the distance of the deeper quencher from the center of the bilayer) is 12.15 and 7.65 Å, as described before.[18]

Order and Packing Studies by X-ray Scattering Measurements. The preparation of the lipid dispersions and the X-ray measurements were made as described in previous works.[6,29] Briefly, different quantities of celecoxib and DPPC were dissolved in a chloroform/methanol (3:1, v/v) mixture to obtain the required molar fractions of the drug (10, 20, and 40 mol %). These solutions were dried under a nitrogen stream to form lipid films. In order to remove all traces of the organic solvents, the lipid films were left overnight under reduced pressure. The hydration of the lipid films was made by adding hepes or acetate buffer, heating in a water bath at 60 °C (temperature above the main phase transition of the lipid), vortexing for about 5 min, and centrifuging for 30 s at 2000 g. This procedure was repeated three times to ensure that all lipid film was hydrated. The samples were aged overnight at 4 °C and vortexed at room temperature for 5 min. The dispersions were transferred into X-ray transparent glass capillaries with 1.5 mm diameter (Hilgenberg, Malsfeld, Germany), which were sealed using a flame and stored at 4 °C until measurement.

SAXS and WAXS measurements were performed at the beamline A2 at Doris III of HASYLAB (DESY, Hamburg, Germany) using monochromatic radiation with a wavelength of 0.15 nm. The SAXS and WAXS detectors were calibrated with rat-tail tendon (RTT) and by poly(ethylene terephthalate) (PET), respectively. Static exposures were taken at temperatures below (20 and 38 °C) and above (50 °C) the main transition temperature, and heating scans were performed at a

dx.doi.org/10.1021/jp304037v | J. Phys. Chem. B XXXX, XXX, XXX–XXX

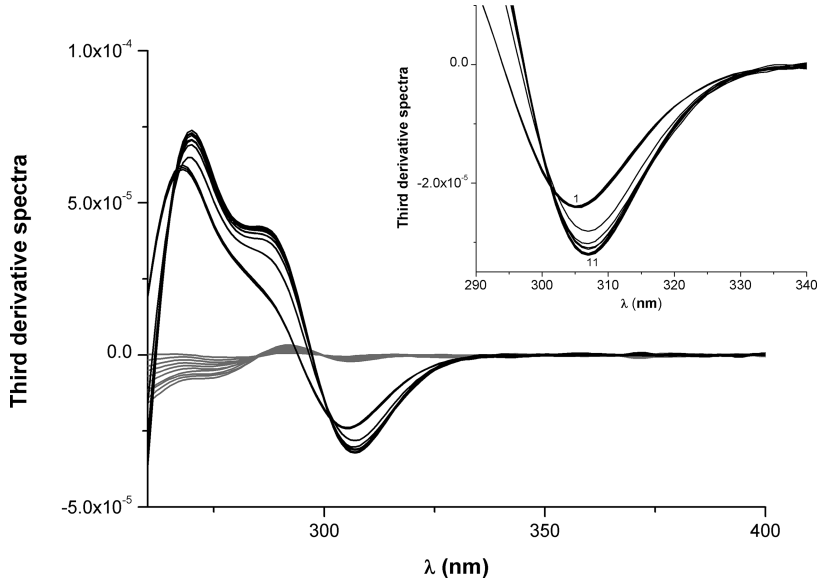

Figure 1. Third derivative of the absorption spectra of celecoxib (20 μM) incubated in LUVs of DMPC (black lines) and LUVs of DMPC without drug (gray lines) at different lipid concentrations from 0 (1) to 1 × 10^{-3} (11) mol L^{-1} at 30 °C and at pH 5.0. The inset graph represents the absorption spectra of DMPC LUVs in the presence of celecoxib around the minimum wavelength of 305 nm.

rate of 1 °C min^{-1} at the range 10−60 °C. After each temperature step, the sample was allowed to equilibrate for 5 min before the diffraction pattern was recorded, and then data were recorded for 10 s every minute. A shutter mounted before the sample was kept closed when no data were acquired in order to minimize the X-ray exposure to the sample. Each diffraction pattern is presented as normalized scattering intensity in arbitrary units versus the reciprocal spacing s (s = (2 sin θ)/λ, where θ is the diffraction angle and λ is the X-ray wavelength). The diffraction peaks obtained were fitted with Lorentzians. The positions of maximum intensity and the full widths of the peaks at one-half of their intensity (fwhm) were determined and used to calculate the correlation length between the lipid bilayers ($\xi = 2\pi$/fwhm). The repeat distances, d ($d = 1/s$) were calculated from the peak maximum positions of the diffraction patterns. Errors in experimental values of d and ξ were assessed based on error estimates of the partial molecular volumes of DPPC and water.[30]

RESULTS AND DISCUSSION

Determination of Partition Coefficient of Celecoxib by Derivative Spectrophotometry. Lipophilicity greatly influences the drugs' pharmacokinetic and pharmacodynamic profiles. Indeed, drugs need to pass through several biological membranes, usually by passive diffusion processes, in order to be absorbed, distributed, metabolized, and eliminated. The partition coefficient (K_p) is a way to measure the lipophilicity of drugs, by studying the drug distribution between aqueous and lipid phases. Therefore, its determination facilitates the prediction and understanding of drug passive diffusion processes and justifies the enormous importance of this physicochemical property in medicinal chemistry.[31] The determination of partition coefficient is of particular importance for the study of NSAIDs, as it influences their resorption from the upper GI tract and may affect their local gastromucosal tolerability and ultimately affects their bodily distribution and efficacy to reach the membrane-associated enzyme COX.[29,32,33]

Therefore, we used UV−vis derivative spectrophotometry to determine celecoxib partition coefficient, as this method has the advantage of not requiring phase separation, and thus, the equilibrium established between the drug and the membrane is not disturbed.[34] However, it is necessary to use a derivative method due to the strong background signals that arise from the light scattered by liposomes. Indeed, the third derivation of spectra eliminates this background signal and improves the resolution of the absorption signals by sharpening the bands.[23,35]

Figure 1 is an example of the third-derivative absorbance spectra of celecoxib with different concentrations of LUVs of DMPC at pH 5.0 and 30 °C (fluid phase). By calculating the third-derivative spectra from celecoxib absorption spectra, it was possible to eliminate the LUVs background signal at celecoxib minimum wavelength (λ_{min}) of 305 nm. Moreover, it is possible to observe a shift of 4 nm in the λ_{min} with increasing lipid concentrations (see the inset graph in Figure 1). This bathochromic shift, observed with the addition of increasing lipid concentration, is a proof that the polarity of the environment surrounding the compound has changed with a clear indication of its partition within the lipid media.[24,36]

K_p was determined by fitting eq 1 to third-derivative spectra of celecoxib at λ_{min} of 305 nm, where the background signal was eliminated, using a nonlinear least-squares regression method (see as an example Figure 2).

The liposomes/water partition coefficients of celecoxib were determined at two different pH values (5.0 and 7.4) and at 30 °C, temperature at which DMPC is in the fluid phase. The results obtained expressed as log D are listed in Table 1.

The analysis of Table 1 reveals that celecoxib liposome/water partition is quite similar for both pH values studied. Celecoxib has a pK_a of 11.1[37,38] and therefore, by using *Marvin Sketch Calculator* (v 5.8.0) software from Chemaxon, it is possible to predict that approximately 100% of celecoxib molecules are in the neutral form at pH 5.0 and 7.4. The same software was used to calculate octanol/water log D of celecoxib at both pH values. For either pH value, the log D calculated is 4.01, which is consistent with the experimental results obtained. The

dx.doi.org/10.1021/jp304037v | J. Phys. Chem. B XXXX, XXX, XXX−XXX

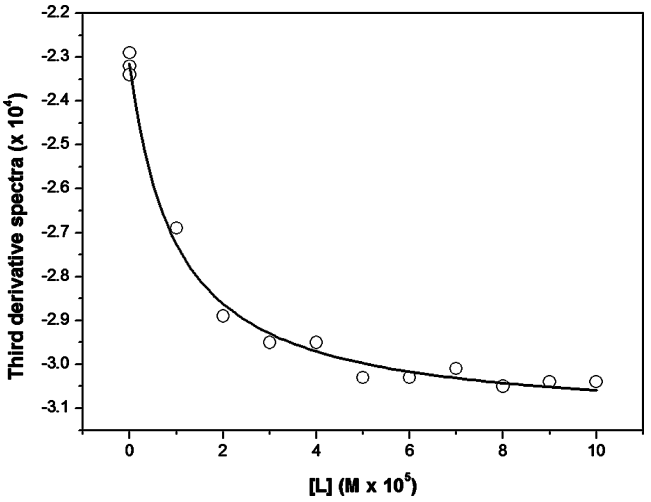

Figure 2. Third-derivative spectra data collected at minimum wavelength of 305 nm for celecoxib at different concentrations of LUVs of DMPC. The line represents the best fit to eq 1.

Table 1. Partition Coefficients (log *D*) (Dimensionless) of Celecoxib in LUVs of DMPC at pH 5.0 and 7.4 and at 30 °C[a]

pH	log *D*
5.0	4.2 ± 0.1
7.4	4.3 ± 0.1

[a]Results present the mean and standard deviation of at least three independent essays.

similarity between octanol/water and liposome/water partition coefficients indicates that the distribution of celecoxib in LUVs of DMPC is mainly driven by hydrophobic interactions. Indeed, if any other type of interaction was involved in the distribution of celecoxib at the membrane level (e.g., electrostatic interactions), the octanol/water system would not be able to predict the contribution of these interactions, as there are no polar mimetic groups on this biphasic system, and there would be expected differences in the partition coefficients determined in this biphasic system or in a lipid/water system. The prevalence of hydrophobic interactions established between drug and membrane can be explained by the fact that celecoxib is predominantly in the neutral form at both pH values, which leads to a similar partition behavior of celecoxib at both pH conditions. This result indicates that celecoxib should preferentially interact with the hydrophobic core of liposomes and is in agreement with other studies of interaction of celecoxib with β-cyclodextrins (β-CD), where the tendency of this NSAID to complex with β-CD in aqueous solution was mainly driven by the hydrophobic effect.[39]

Effects of Celecoxib in Membrane Phase Transition Parameters. The study of the main phase transition temperature (T_m) of lipids, from gel phase to fluid phase, is crucial when analyzing the biophysical properties of membranes. Indeed, this lipid transition has great impact on order and fluidity of membranes and depends on temperature, hydration, and lipid composition.[31] In this regard, several techniques have been described to determine the lipids' phase transition temperatures, such as differential scanning calorimetry (DSC), fluorescence anisotropy, Fourier transform infrared spectroscopy (FTIR), and nuclear magnetic resonance (NMR). However, these methods are far from ideal in a routine study by requiring complex instrumentation, exogenous probes, or modified compounds or solvents. In this context, the determination of lipid transition temperatures by dynamic light scattering (DLS) has advantages, since the system equilibrium is not perturbed by an exogenous compound and the instrumentation is simple and common in biophysical facilities where it is required for the characterization of liposomes and other nanoparticles. This technique is based on the fact that the average count rate (average number of photons scattered detected per second) measured by a DLS instrument reflects changes in the optical properties of lipids during temperature variations.[26]

The temperature dependence of DMPC average count rate in the presence and absence of celecoxib at pH 7.4 is shown in Figure 3. From the sigmoidal inflection point of the

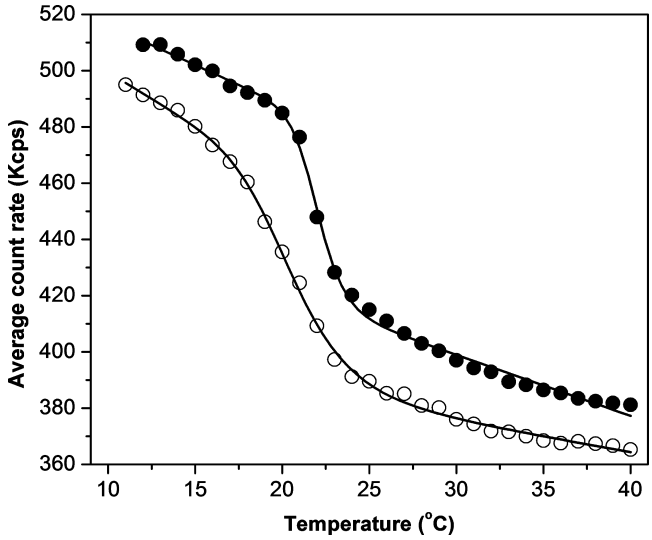

Figure 3. Average count rate of DMPC liposomes in the absence (solid symbols) and presence (open symbols) of celecoxib at pH 7.4 as a function of temperature. Continuous lines are the best fit curves using eq 2.

experimental data obtained, it was possible to calculate the T_m of DMPC vesicles and the cooperativity of the transition by fitting the experimental data with eq 2.[27] The results obtained for both pH values and systems studied are presented in Table 2.

Table 2. Values of Main Phase Transition Temperature (T_m) and Cooperativity (B) Obtained for LUVs of DMPC in the Absence and Presence of Celecoxib at pH 5.0 and 7.4

	pH	T_m (°C)	B
DMPC	5.0	22.0 ± 0.1	345 ± 25
DMPC + Celecoxib		21.7 ± 0.1	214 ± 4
DMPC	7.4	22.0 ± 0.4	209 ± 52
DMPC + Celecoxib		20.7 ± 0.3	132 ± 81

At pH 5.0, the incorporation of celecoxib affected the cooperativity of the transition but not the T_m of DMPC vesicles. In contrast, at pH 7.4, celecoxib lowered the T_m of pure DMPC by around 1 °C and also lowered the transition cooperativity. The alteration of these parameters immediately demonstrates the disturbing effect of celecoxib on membrane order, due to the location of this drug within the DMPC

dx.doi.org/10.1021/jp304037v | J. Phys. Chem. B XXXX, XXX, XXX−XXX

bilayer. Furthermore, the meticulous analysis of the celecoxib effect on the cooperativity and T_m parameters gives some indication about the location of this drug within the lipid bilayer. In fact, the qualitative and quantitative differences in the lipid phase transition characteristics arise from a location of the molecules in different regions of the bilayer. The deeper region of the lipid bilayer (corresponding to the acyl chains from the C9 to C14 region) is less ordered than the shallower region near the head groups of the phospholipids (corresponding to the acyl chains from C1 to C8 region).[22] In this context, the less ordered region of membranes is the least perturbed by drugs that are located in this region, because its fluid-like nature is able to better accommodate foreign molecules. Hence, any changes in the transition parameters such as cooperativity or T_m are largely regulated by the interaction with the cooperative unit constituted by carbons 1 to 8 of the acyl chains, where the membrane is more ordered.[40] It is therefore suggested that the greater changes in the cooperativity and T_m induced by celecoxib at pH 7.4 indicate a shallower membrane location of the drug. On the other hand, at pH 5.0 celecoxib induces less membrane perturbing effects, which may be a sign of this NSAID's deeper location in the disordered region of the membrane.

Membrane Binding and Membrane Location of Celecoxib Evaluated by Fluorescence Quenching Studies. The determination of membrane location of drugs is crucial when studying drug–membrane interactions, in order to understand the therapeutic and toxic effects of drugs. Fluorescence quenching is a relevant technique to analyze the membrane location of drugs, since the accessibility of a fluorophore to a quencher can indicate its position in a membrane. Therefore, if the molecular location of a quencher within the membrane is well-characterized, quenching studies can be performed to reveal the membrane location of a fluorophore or the membrane accessibility to a fluorophore.[41]

In this work, *n*-DOXYL labeled liposomes were used as quenchers, since the location of DOXYL group within the membrane is known with certainty. It was demonstrated that 5-DOXYL is located near the surface, while 10-DOXYL locates deeper in the hydrocarbon core of the membrane.[18] The fluorescent drug, celecoxib, was used as a fluorophore, and increasing concentrations of this NSAID were incubated with *n*-DOXYL labeled liposomes. The changes in celecoxib fluorescence emission upon binding to lipid membrane (ΔF) were obtained by subtracting the fluorescence at each concentration of drug added to *n*-DOXYL-labeled liposomes from the initial fluorescence of the reference samples containing the same drug concentration added to liposomes without *n*-DOXYL probe. The fluorescence changes detected upon titration of the labeled vesicles with celecoxib (ΔF) are a sign of the drug binding to the membrane, and this binding behavior is described by the different binding isotherm plots displayed in Figure 4.

The binding isotherms were obtained by a nonlinear curve fitting of eq 3 to a scatter plot of the ΔF values as a function of celecoxib concentration, where the adjustable parameters are the maximum quenching effect (ΔF_{max}) and the dissociation constant (K_D). From the calculated dissociation constant (K_D), it is possible to determine the binding constant, K_B ($K_B = 1/K_D$), that translates the affinity of celecoxib to enter the lipid membrane (Table 3).

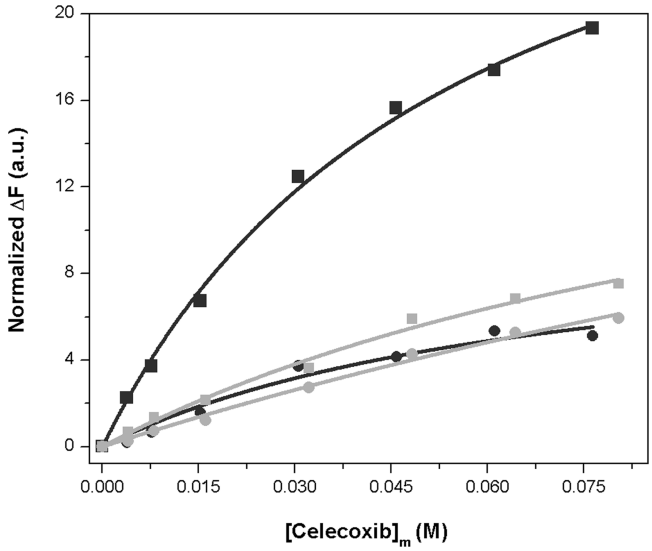

Figure 4. Binding isotherms of LUVs of DMPC labeled with 5-DOXYL (squares) and 10-DOXYL (circles) upon addition of celecoxib at pH 5.0 (dark gray) and 7.4 (light gray).

Table 3. Binding Constants (K_B) of Celecoxib to Membrane and Celecoxib Penetration Depth (Z_{cf})

		$K_B \times 10^4$	Z_{cf} (Å)
pH 5.0	5-DOXYL	6.8 ± 0.3	3.9 ± 0.5
	10-DOXYL	62 ± 3	
pH 7.4	5-DOXYL	32 ± 2	12.1 ± 0.3
	10-DOXYL	13.1 ± 0.7	

The distance between celecoxib and the center of the membrane was determined according to eq 5, and the results are also presented in Table 3.

Results show that the depth of celecoxib in the membrane is pH-dependent. At pH 5.0, celecoxib penetrates deeper in the membrane than at pH 7.4. In fact, when comparing the Z_{cf} values of celecoxib (Table 3) to the ones of the nitroxide probes (12.15 Å for 5-DOXYL and 7.65 Å for 10-DOXYL), it is possible to observe that at pH 7.4 celecoxib is at about the same depth in the membrane as 5-DOXYL, which means that celecoxib is located very near C5 of the hydrophobic region of the membrane. Furthermore, this result is also supported by the higher binding constant obtained with 5-DOXYL than with 10-DOXYL at pH 7.4, which consistently indicates that celecoxib–membrane binding occurs more efficiently at the shallower region of the membrane. On the other hand, and once that the Z_{cf} value at pH 5.0 is smaller than for the probe 10-DOXYL, celecoxib is located even deeper than 10-DOXYL, pointing to a location beneath the C10 of the hydrophobic chains. Once again, the binding constants are in agreement with the stated conclusion, since at pH 5.0, celecoxib K_B is significantly higher with 10-DOXYL, suggesting that the drug is located deep inside the bilayer. These results are in good agreement with the previously described effects of celecoxib in lipid phase transition temperature that point to the same conclusions, i.e., celecoxib has a deeper membrane penetration at pH 5.0 than at pH 7.4.

Effects of Celecoxib in Lipid Order and Packing Evaluated by X-ray Scattering Studies. The study of the X-ray patterns of DPPC bilayers at small and wide angles in the presence and absence of celecoxib permits to obtain information about the long-range bilayer organization and the

dx.doi.org/10.1021/jp304037v | J. Phys. Chem. B XXXX, XXX, XXX–XXX

Table 4. Long Distances (d) and Correlation Length (ξ) Determined from First-order Bragg Peaks of SAXS Diffraction Patterns at pH 5.0 and 7.4 and at 20, 38, and 50 °C[a]

		pH 5.0			pH 7.4		
	$\chi_{celecoxib}$	0	10	20	0	10	20
20 °C ($L_{\beta'}$)	d_1	64.9 ± 0.5	73.2 ± 0.5	73.7 ± 0.5	63.5 ± 0.5	72.4 ± 0.5	72.7 ± 0.5
	ξ_1	528 ± 10	350 ± 10	342 ± 10	989 ± 10	753 ± 10	553 ± 10
	d_2	-	57.7 ± 0.5	61.5 ± 0.5	-	62.1 ± 0.5	61.7 ± 0.5
	ξ_2	-	98 ± 10	134 ± 0	-	200 ± 10	271 ± 10
38 °C ($P_{\beta'}$)	d_1	75.8 ± 0.5	75.9 ± 0.5	74.7 ± 0.5	71.7 ± 0.5	72.3 ± 0.5	72.5 ± 0.5
	ξ_1	470 ± 10	495 ± 10	576 ± 10	706 ± 10	473 ± 10	552 ± 10
	d_2	62.9 ± 0.5	59.8 ± 0.5	-	66.3 ± 0.5	65.3 ± 0.5	67.1 ± 0.5
	ξ_2	156 ± 10	96 ± 10	-	276 ± 10	259 ± 10	295 ± 10
50 °C (L_{α})	d_1	73.2 ± 0.5	74.3 ± 0.5	74.1 ± 0.5	67.0 ± 0.5	67.0 ± 0.5	66.9 ± 0.5
	ξ_1	206 ± 10	711 ± 10	728 ± 10	762 ± 10	801 ± 10	518 ± 10
	d_2	-	68.5 ± 0.5	68.5 ± 0.5	-	-	-
	ξ_2	-	281 ± 0.5	98 ± 10	-	-	-

[a]The data are presented in Å as a function of the mol % of celecoxib.

hydrocarbon chain packing, respectively. In fact, the organization and packing of DPPC phospholipids are temperature dependent, and it has already been described that NSAIDs are able to induce changes in lipid packing, order, and hydration layer, and the magnitude of these changes are dependent on the lipid phase.[6,8,29]

The interaction of celecoxib with the DPPC bilayers was studied by SAXS and WAXS at 20, 38, and 50 °C, temperatures at which DPPC is organized in the gel phase ($L_{\beta'}$), ripple gel phase ($P_{\beta'}$), and fluid phase (L_{α}), respectively. For pure DPPC and at both pH values, the SAXS data demonstrate the existence of lamellar structures at the $L_{\beta'}$, $P_{\beta'}$, and L_{α} phases, with d values (see Table 4) that are in good agreement with those in the literature.[6,29]

In the $L_{\beta'}$ phase, the presence of celecoxib drastically changes the SAXS diffraction pattern at both pH values, as can be seen for pH 7.4 in Figure 5.

In fact, it can be observed in Figure 5 and in Table 4 that at 20 °C the presence of celecoxib induces the appearance of two Bragg peaks with repeated distances that are similar to the typical peaks of pure DPPC in the ripple phase. The $P_{\beta'}$ phase occurs due to structural constraints between the packing characteristics of the two acyl chains and the headgroup, and for pure DPPC, the typical pretransition (from $L_{\beta'}$ to $P_{\beta'}$) temperature is 34.5 °C (at pH 7.4).[29] The presence of celecoxib induces the earlier formation of a metastable ripple phase that can be seen even at 10 °C, for both pH conditions (data not shown). The presence of a ripple phase at temperatures at which a more packed gel phase was expected suggests that celecoxib has a disordering effect on the lipid bilayers. Consistently, the WAXS profiles presented in Figure 6 clearly show that at pH 5.0 the pattern obtained for pure DPPC at 38 °C is very similar to the ones obtained for the different molar fractions of celecoxib at 20 °C. The same behavior is observed at pH 7.4 (data not shown). In fact, the presence of celecoxib leads to a change from the orthorhombic chain packing to the typical hexagonal packing of the ripple phase, which is demonstrated by the existence of just one Bragg peak on the WAXS patterns at 20 °C (Figure 6).

At 38 °C, at pH 5.0 and as far as long distances are concerned, the effect of celecoxib is dependent on its molar fraction. For 10 mol % fraction, the two typical peaks of the ripple phase are maintained, whereas for 20 mol %, the Bragg peak positions indicate that the bilayers are already at the fluid phase, although with some phase separation. At pH 7.4, there is no indication of the DPPC transition for the L_{α} phase even for the highest molar fraction studied. However, the disturbing effect of celecoxib is demonstrated by the decrease of the cooperativity of the first-order peak. At pH 5.0, the WAXS profile for the mixtures of DPPC with celecoxib (see Figure 6) presents a very broad peak characteristic of the L_{α} phase. On the other hand, at pH 7.4, although the process is much less cooperative, it is still possible to fit a peak with a distance typical of the $P_{\beta'}$ phase (data not shown).

At 50 °C and at pH 5.0, the existence of a broad peak that can be deconvoluted in two peaks can be observed (Table 4), when celecoxib is present. The existence of two repeated distances indicates that the drug is not homogenously distributed in the membrane and there are two different phases, one noninfluenced phase (first peak that is approximately at the same position as the peak of the pure DPPC) and one phase influenced by celecoxib (second peak). Once there is a decrease of the d value of the second peak relative to that of pure DPPC, this result might be interpreted in terms of a reduction of the hydration layer that is usually enhanced at the fluid phase. At pH 7.4 and for the L_{α} phase, the interference of celecoxib on the long-range bilayer order is shown by the reduction of the cooperativity of the first-order peak for the highest molar fraction used.

To further access the effect of celecoxib in the membrane phase transition temperature, the SAXS repeated distances corresponding to the position of first-order Bragg peaks was plotted as a function of temperature for the systems of DPPC with 10 mol % of celecoxib at pH 5.0 and 7.4. This plot renders a sigmoidal profile (Figure 7), in which the midpoint represents the main phase transition temperature (T_m).

Equation 2 was used to fit to the profiles obtained in Figure 7 in order to determine T_m, which was calculated as an average between the obtained values. In this view, at pH 7.4 the T_m for DPPC + 10 mol % of celecoxib is (38.9 ± 0.5) °C, and at pH 5.0, it is (38.0 ± 0.5) °C. These results are in good agreement with the WAXS experiments, where the scans of WAXS patterns at several temperatures point to about the same T_m values (data not shown).

Besides evaluating the effect of celecoxib on T_m, it is also possible to observe in Figure 7 that this coxib has abolished the pretransition temperature (T_p), since there is no other inflection point on the sigmoidal plot besides the one

dx.doi.org/10.1021/jp304037v | J. Phys. Chem. B XXXX, XXX, XXX−XXX

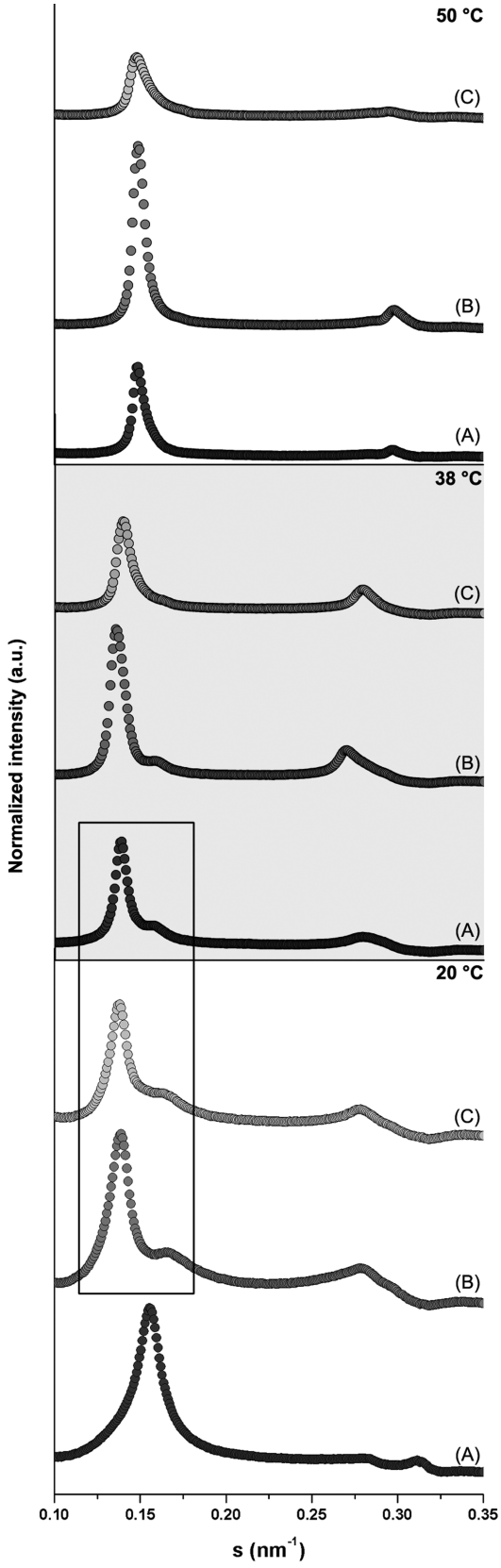

Figure 5. Small-angle X-ray diffraction profiles at 20, 38, and 50 °C for DPPC (A) and mixtures of DPPC with celecoxib at 10 mol % (B) and 20 mol % (C) at pH 7.4. The box highlights the similarity of the diffraction patterns of DPPC with celecoxib at 20 °C with the diffraction pattern of pure DPPC at 38 °C.

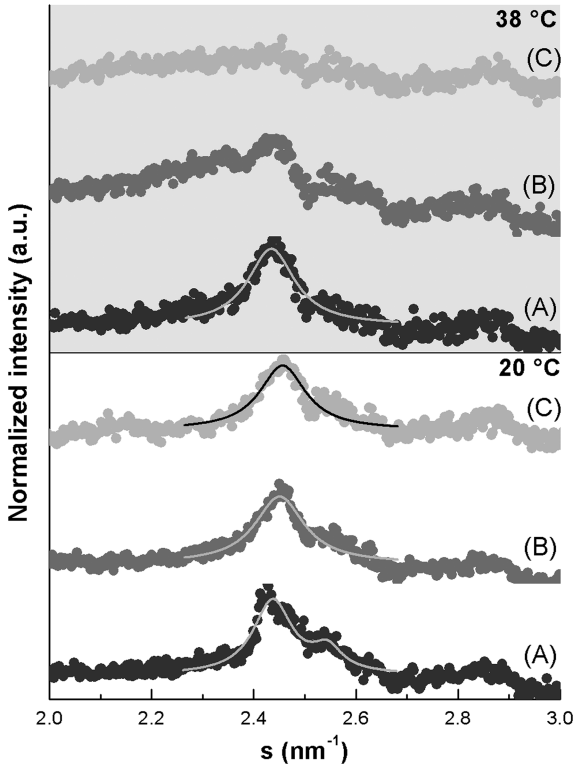

Figure 6. Wide-angle X-ray diffraction profiles at 20 and 38 °C for DPPC (A) and mixtures of DPPC with celecoxib at 10 mol % (B) and 20 mol % (C) at pH 5.0.

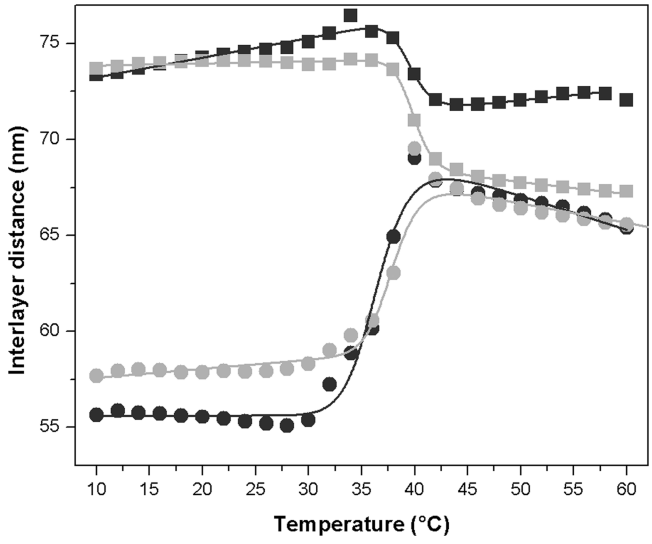

Figure 7. Temperature dependence of the lamellar lattice constants d_1 (squares) and d_2 (circles) at pH 5.0 (dark gray) and pH 7.4 (light gray) for mixtures of DPPC with celecoxib at 10 mol %.

corresponding to the main phase transition temperature. This corroborates the previous assumption that celecoxib has a disordering effect on the membrane, inducing the presence of a ripple phase even at low temperatures such as 10 °C at which a more packed gel phase was expected.

CONCLUSIONS

The results obtained in this work point to a great interaction of celecoxib with membranes. In fact, we have obtained a high and

dx.doi.org/10.1021/jp304037v | J. Phys. Chem. B XXXX, XXX, XXX−XXX

non-pH-dependent celecoxib partition coefficient with membranes, and the results have also indicated that celecoxib−membrane interaction occurs essentially by hydrophobic interactions. These results are in good agreement with the high therapeutic efficiency of celecoxib, since the drug accumulation in membranes leads to higher concentrations at the active site of COX-2 than in the surrounding aqueous phase. In contrast, the location of celecoxib within the membrane is pH-dependent according to both main phase transition temperature and location studies results. Indeed, celecoxib is located deeper inside the membrane at pH 5.0 and closer to the surface at pH 7.4. Again, this *in vitro* deeper membrane location of celecoxib at pH 5.0 can translate to an analogous deeper location of celecoxib in inflamed cells which present similar slight acidic pH values. This deeper location of celecoxib in inflamed cell membranes might constitute an advantage of celecoxib being able to reach the active site of COX-2, and consequently facilitating the anti-inflammatory effects of celecoxib.

It has already been described for several NSAIDs that their topical effect on the stomach mucus protective layer at acidic pH can be a factor to explain their adverse gastrointestinal effects.[6,7,42] However, concerning celecoxib, its membrane location closer to the center of the bilayer at pH 5.0 might be an additional explanation for its low adverse GI effects. Indeed, membranes possessing a fluidity gradient are much less ordered and less prone to perturbations at their core. Therefore, the deeper the drug location, the smaller the drug influence on the biophysical properties of phospholipids.[40]

Even though celecoxib is not responsible for GI injuries, it is still associated with adverse cardiovascular effects, and despite their severity, the mechanisms underlying these effects are not completely clarified. In this regard, the high disordering effect of celecoxib toward membranes observed by SAXS and WAXS measurements might be a factor to take into consideration. In fact, it has already been described that the drug-induced modification of cardiovascular membrane systems in terms of structure and lipid composition can result in cardiovascular hazards.[4] The increase of the fluidization of cardiovascular system membranes might be related with alterations of enzyme activities and modification of membrane permeability, which might ultimately lead to cardiovascular diseases. Accordingly, celecoxib has been reported to affect the calcium homeostasis by interacting with calcium ATPases,[43] and the membrane fluidization induced by this drug might be a factor for the impairment of ATPase function. Furthermore, the current study supports the assumption that the role of membrane biophysics is a key factor to understand celecoxib adverse cardiovascular effects, and according to this study, the greater membrane disordering effects of celecoxib were detected at pH 7.4, where the drug has a shallower location consistent with the type of membrane location and biophysical impairment observed in cases of cardiovascular adverse effects.

Besides being used in the treatment of rheumatic diseases, celecoxib was also approved for the adjuvant treatment of familial adenomatous polyposis because of its antitumor effects. It has been documented that membrane fluidization of some drugs is related with their therapeutic efficiency in inducing apoptosis.[44] Therefore, the high membrane disordering effect demonstrated by celecoxib in this work can be associated with the reported modification of calcium homeostasis, and both these effects might play a role in the apoptotic effect of celecoxib.[43]

In conclusion, the research described herein signifies a well-characterized celecoxib−membrane interaction study, exploiting the effects of this coxib on membrane biophysical properties. Besides unveiling the mechanisms of interaction of celecoxib with membranes, this work can contribute to identifying novel biophysical explanations for NSAID toxicity and therapeutic effects, hence allowing the future development of more selective drugs, diminishing the undesirable side effects.

AUTHOR INFORMATION

Corresponding Author

*Tel: +351 220428672. Fax: +351 226093483. E-mail address: cdnunes@ff.up.pt.

Present Address

Rua de Jorge Viterbo Ferreira, 228, 4050−313 Porto, Portugal.

Notes

The authors declare no competing financial interest.

ACKNOWLEDGMENTS

C.N. thanks FCT (Fundação para a Ciência e Tecnologia) for the Post-Doctoral Grant (SFRH/BPD/81963/2011). The authors also thank HASYLAB at DESY, Hamburg, Germany, for beam time and support through the project II-20100139 EC.

REFERENCES

(1) Frampton, J. E.; Keating, G. M. *Drugs* **2007**, *67*, 2433−2472.
(2) Sweetman, S. *Martindale: The Complete Drug Reference*; Pharmaceutical Press: London, 2011.
(3) Laine, L.; Curtis, S. P.; Cryer, B.; Kaur, A.; Cannon, C. P. *Lancet* **2007**, *369*, 465−473.
(4) Escriba, P. V. *Trends Mol. Med.* **2006**, *12*, 34−43.
(5) Lichtenberger, L. M.; Zhou, Y.; Dial, E. J.; Raphael, R. M. *J. Pharm. Pharmacol.* **2006**, *58*, 1421−1428.
(6) Nunes, C.; Brezesinski, G.; Lima, J. L. F. C.; Reis, S.; Lucio, M. *J. Phys. Chem. B* **2011**, *115*, 8024−8032.
(7) Nunes, C.; Brezesinski, G.; Lopes, D.; Lima, J. L. F. C.; Reis, S.; Lucio, M. *J. Phys. Chem. B* **2011**, *115*, 12615−12623.
(8) Nunes, C.; Brezesinski, G.; Pereira-Leite, C.; Lima, J. L. F. C.; Reis, S.; Lucio, M. *Langmuir* **2011**, *27*, 10847−10858.
(9) Gaspar, D.; Lucio, M.; Rocha, S.; Lima, J. L. F. C.; Reis, S. *Chem. Phys. Lipids* **2011**, *164*, 292−299.
(10) Gaspar, D.; Lucio, M.; Wagner, K.; Brezesinski, G.; Rocha, S.; Costa Lima, J. L. F.; Reis, S. *Biophys. Chem.* **2010**, *152*, 109−117.
(11) Escriba, P. V.; Gonzalez-Ros, J. M.; Goni, F. M.; Kinnunen, P. K. J.; Vigh, L.; Sanchez-Magraner, L.; Fernandez, A. M.; Busquets, X.; Horvath, I.; Barcelo-Coblijn, G. *J. Cell Mol. Med.* **2008**, *12*, 829−875.
(12) Butoescu, N.; Jordan, O.; Doelker, E. *Eur. J. Pharm. Biopharm.* **2009**, *73*, 205−218.
(13) Shinitzky, M. *Biomembranes: Physical Aspects*; Wiley-VCH: Weinheim, 1996.
(14) Lucio, M.; Nunes, C.; Gaspar, D.; Golebska, K.; Wisniewski, M.; Lima, J. L. F. C.; Brezesinski, G.; Reis, S. *Chem. Phys. Lett.* **2009**, *471*, 300−309.
(15) Lucio, M.; Ferreira, H.; Lima, J. L. F. C.; Reis, S. *Redox Rep.* **2008**, *13*, 225−236.
(16) Gautam, M.; Benson, C. J.; Sluka, K. A. *Neuroscience* **2010**, *170*, 893−900.
(17) Kondo, M.; Mehiri, M.; Regen, S. L. *J. Am. Chem. Soc.* **2008**, *130*, 13771−13777.
(18) Chattopadhyay, A.; London, E. *Biochemistry* **1987**, *26*, 39−45.
(19) Harroun, T. A.; Kucerka, N.; Nieh, M. P.; Katsaras, J. *Soft Matter* **2009**, *5*, 2694−2703.
(20) Brittes, J.; Lucio, M.; Nunes, C.; Lima, J. L.; Reis, S. *Chem. Phys. Lipids* **2010**, *163*, 747−754.

(21) Lucio, M.; Bringezu, F.; Reis, S.; Lima, J. L. F. C.; Brezesinski, G. *Langmuir* **2008**, *24*, 4132−4139.
(22) Lucio, M.; Ferreira, H.; Lima, J. L. F. C.; Matos, C.; de Castro, B.; Reis, S. *Phys. Chem. Chem. Phys.* **2004**, *6*, 1493−1498.
(23) Ferreira, H.; Lucio, M.; de Castro, B.; Gameiro, P.; Lima, J. L. F. C.; Reis, S. *Anal. Bioanal. Chem.* **2003**, *377*, 293−298.
(24) Magalhaes, L. M.; Nunes, C.; Lucio, M.; Segundo, M. A.; Reis, S.; Lima, J. L. F. C. *Nat. Protoc.* **2010**, *5*, 1823−1830.
(25) Marsh, D. *Handbook of Lipid Bilayers*; CRC Press: Göttingen, 2012.
(26) Michel, N.; Fabiano, A. S.; Polidori, A.; Jack, R.; Pucci, B. *Chem. Phys. Lipids* **2006**, *139*, 11−19.
(27) Grancelli, A.; Morros, A.; Cabanas, M. E.; Domenech, O.; Merino, S.; Vazquez, J. L.; Montero, M. T.; Vinas, M.; Hernandez-Borrell, J. *Langmuir* **2002**, *18*, 9177−9182.
(28) Chen, X. Y.; Wolfgang, D. E.; Sampson, N. S. *Biochemistry* **2000**, *39*, 13383−13389.
(29) Nunes, C.; Brezesinski, G.; Lima, J. L. F. C.; Reis, S.; Lucio, M. *Soft Matter* **2011**, *7*, 3002−3010.
(30) Greenwood, A. I.; Tristram-Nagle, S.; Nagle, J. F. *Chem. Phys. Lipids* **2006**, *143*, 1−10.
(31) Seydel, J. K.; Wiese, M. *Drug-Membrane Interactions: Analysis, Drug Distribution, Modeling*; Wiley-VCH: Weinheim, 2003.
(32) Kyrikou, I.; Hadjikakou, S. K.; Kovala-Demertzi, D.; Viras, K.; Mavromoustakos, T. *Chem. Phys. Lipids* **2004**, *132*, 157−169.
(33) Więcław, K.; Korchowiec, B.; Corvis, Y.; Korchowiec, J.; Guermouche, H.; Rogalska, E. *Langmuir* **2009**, *25*, 1417−1426.
(34) Santos, N. C.; Prieto, M.; Castanho, M. A. R. B. *Biochim. Biophys. Acta: Biomembr.* **2003**, *1612*, 123−135.
(35) Kitamura, K.; Imayoshi, N.; Goto, T.; Shiro, H.; Mano, T.; Nakai, Y. *Anal. Chim. Acta* **1995**, *304*, 101−106.
(36) de Castro, B.; Gameiro, P.; Lima, J. L. F. C.; Matos, C.; Reis, S. *Lipids* **2001**, *36*, 89−96.
(37) Reddy, M. N.; Rehana, T.; Ramakrishna, S.; Chowdary, K. P. R.; Diwan, P. V. *Aaps PharmSci* **2004**, *6*.
(38) Paulson, S. K.; Vaughn, M. B.; Jessen, S. M.; Lawal, Y.; Gresk, C. J.; Yan, B.; Maziasz, T. J.; Cook, C. S.; Karim, A. *J. Pharmacol. Exp. Ther.* **2001**, *297*, 638−645.
(39) Omari, M.; Zughul, M.; Davies, J.; Badwan, A. *J. Inclusion Phenom. Macrocyclic Chem.* **2006**, *55*, 247−254.
(40) Liu, Q.; Qu, Y.; Van Antwerpen, R.; Farrell, N. *Biochemistry* **2006**, *45*, 4248−4256.
(41) Lakowicz, J. R. *Principles of Fluorescence Spectroscopy*; Springer: New York, 2006.
(42) Lichtenberger, L. M. *Biochem. Pharmacol.* **2001**, *61*, 631−637.
(43) Johnson, A. J.; Hsu, A. L.; Lin, H. P.; Song, X. Q.; Chen, C. S. *Biochem. J.* **2002**, *366*, 831−837.
(44) Rebillard, A.; Tekpli, X.; Meurette, O.; Sergent, O.; LeMoigne-Muller, G.; Vernhet, L.; Gorria, M.; Chevanne, M.; Christmann, M.; Kaina, B.; et al. *Cancer Res.* **2007**, *67*, 7865−7874.